



ASME Accepted Manuscript Repository

Institutional Repository Cover Sheet

Cranfield Collection of E-Research - CERES

ASME Paper

Title: Design methodology and mission assessment of parallel hybrid electric propulsion systems

Authors:

Raj Ghelani, Ioannis Roumeliotis, Chana Anna Saias, Christos Mourouzidis, Vassilios Pachidis,
Justin Norman, Marko Bacic

ASME Journal

Title: Journal of Engineering for Gas Turbines and Power

Volume/Issue: AAM Available online 16 September 2022 Date of Publication (VOR* Online):

ASME Digital Collection <https://asmedigitalcollection.asme.org/gasturbinespower/article/doi/10.1115/1.4055635/1146249/Design-Methodology-and-Mission-Assessment-of>

DOI: <https://doi.org/10.1115/1.4055635>

*VOR (version of record)

DESIGN METHODOLOGY AND MISSION ASSESSMENT OF PARALLEL HYBRID ELECTRIC PROPULSION SYSTEMS

AUTHORS:

RAJ GHELANI

Centre for Propulsion and Thermal Power Engineering,

Cranfield University, MK43 0AL, UK.

e-mail: R.Ghelani@cranfield.ac.uk

IOANNIS ROUMELIOTIS

Centre for Propulsion and Thermal Power Engineering,

Cranfield University, MK43 0AL, UK.

e-mail: I.Roumeliotis@cranfield.ac.uk

CHANA ANNA SAIAS

Centre for Propulsion and Thermal Power Engineering,

Cranfield University, MK43 0AL, UK.

e-mail: Chana-Anna.Saias@cranfield.ac.uk

CHRISTOS MOUROUZIDIS

Centre for Propulsion and Thermal Power Engineering,

Cranfield University, MK43 0AL, UK.

e-mail: c.mourouzidis@cranfield.ac.uk

VASSILIOS PACHIDIS

Centre for Propulsion and Thermal Power Engineering,

Cranfield University, MK43 0AL, UK.

e-mail: v.pachidis@cranfield.ac.uk

JUSTIN NORMAN

Rolls Royce plc, Derby.

e-mail: Justin.Norman@Rolls-Royce.com

MARKO BACIC

Rolls Royce plc, Derby.

e-mail: Marko.Bacic@Rolls-Royce.com

ABSTRACT

An integrated engine cycle design methodology and mission assessment for parallel hybrid electric propulsion architectures are presented in this paper. The aircraft case study considered is inspired by Fokker 100, boosted by an electric motor on the low-pressure shaft of the gas turbine. The fuel burn benefits arising from boosting the low-pressure shaft are discussed for two different baseline engine technologies.

A three-point engine cycle design method is developed to redesign the engine cycle according to the degree of hybridization. The integrated cycle design and power management optimization method is employed to identify potential fuel burn benefits from hybridization for multiple mission ranges. Genetic algorithm-based optimizer has been used to identify optimal power management strategies. The sensitivity of these mission results has also been analysed for different assumptions on the electric powertrain.

With 1 MW motor power and a battery pack of 2300 kg, a maximum of 3% fuel burn benefit can be obtained by retrofitting the gas turbine for 400 nm mission range. Optimizing the power management strategy can improve this fuel burn benefit by 0.2-0.3%. Redesigning the gas turbine and optimizing the power management strategy, finally provides a maximum fuel benefit of 4.2% on 400 nm.

The results suggest that a high hybridization by power, low hybridization by energy, and ranges below 700 nm are the only cases where the redesigned hybrid electric aircraft has benefits in fuel burn and energy consumption relative to the baseline aircraft.

Finally, it is found that the percentage of fuel burn benefits from the hybrid electric configuration increases with the improvement in engine technology.

NOMENCLATURE

F_N	Thrust
H_E	Degree of hybridization by energy
H_P	Degree of hybridization by power

m_f	Fuel flow
V_j	Jet Velocity ratio
BPR	Bypass ratio
cEIS2035	Conventional entry into service 2035 engine
cTAY	Conventional TAY 651
EOR	End of Runway
FPR	Fan Pressure ratio
hEIS2035	Hybrid entry into service 2035 engine
HEPS	Hybrid electric propulsion systems
HPC	High pressure compressor
hTAY	Hybrid TAY 651
LPC	Low pressure compressor
MCL	Maximum Climb
MCR	Maximum Cruise
MIPH	Mechanically Integrated parallel hybrid
OPR	Overall Pressure ratio
PMS	Power management strategy
PR	Pressure ratio
SoC	State of charge
T/O	Maximum Take-off
Tblade	Turbine blade metal temperature
TSFC	Thrust Specific fuel consumption
UHBR	Ultra-high bypass ratio
WS	Work split IPC/HPC

1. INTRODUCTION

The Advisory Council for Aeronautical Research in Europe (ACARE) has set some ambitious goals for decarbonizing aviation till 2050 [1]. Improvement in the efficiency of current gas turbines and airframes alone will not be sufficient to achieve these goals [2], [3]. Novel propulsion architectures like hybrid electric propulsion systems and alternative fuels are considered for achieving the anticipated leap in fuel efficiency and emissions reduction [2], [4].

In the past decade, NASA has revealed many aircraft configurations, utilizing different novel hybrid electric propulsion architectures. These concepts were namely, N3-X, SUGAR VOLT, and STARC ABL utilizing series/turboelectric, parallel, and partial turboelectric HEPS architectures respectively ([5], [6], [7], [8]). Out of these, parallel hybrid is the most likely solution to be implemented in near future, as other architectures would need MW-class superconducting generators and transmission systems, and newer airframes. Even parallel hybrid electric configurations are not expected to be implemented before the 2030-35 timeframe due to the low power and energy densities of electric batteries and heavy thermal management systems [9]. There has been significant work done in recent years analyzing parallel hybrid propulsion systems for different VTOL ([10], [37]), regional ([11], [12], [13]), UAV [14] and single-aisle narrow-body airframes [15]. Most of the work done on parallel hybrid electric propulsion systems in open literature has been looked at from an aircraft design point of view. The initial study by NASA on the SUGAR VOLT focused on the development of the airframe and electric powertrain models [8]. The work from Mavris et al [16] extended this and conducted analyses at the mission level for a sweep of battery weights on the Refined SUGAR N+4 airframe. The main conclusion from the paper was a 25% fuel burn benefit with a 22500 pounds battery pack on 900 nm at reduced payload relative to the baseline aircraft.

The work of Cees Bil et al [14] and de Vries et al [22] have shown the conceptual design of parallel hybrid electric aircraft without going into the details at an engine cycle level. Trawick [17] produced different ways to assess optimal power management strategies for parallel hybrid architectures. Lents et al [18] focused on the thermal management systems and provided a preliminary approach to engine cycle design by trading bypass ratio with motor power on-take. The work done by Lents et al [18] was the first paper in the open literature that looked at parallel hybrid electric propulsion systems from an engine cycle design point of view. The cycle level benefit from increasing BPR was a 2.3% improvement in TSFC with a 2.1 MW motor. The study also concluded that including the ram-air drag penalty for the electric powertrain cooling system outweighs this benefit. The studies from Sahoo et al [19] and Sielemann et al [20] presented different approaches to cycle design with limited information on its impact at the aircraft mission level. Roumeliotis et al [21] presented the impact of power on-takes on LPC, fan, and HPC operability.

There has been work done on parallel hybrid engine cycle design for a fixed power management strategy as described [18], [19], and [20]. In Lents' study [18], no change is made to the design point FPR and OPR with increasing BPR, and neither the mass flows are conserved at top of climb. This leads to a slight overestimation in fuel burn benefit for the hybrid cycle as the higher drag and weight due to a bigger fan diameter is not accounted for. Another approach was made by Sahoo et al [19] where power on-takes were provided at all the 3 design points, namely, cruise, top of climb, and take-off. The approach was like Lents et al [18], but extra parameters of jet velocity ratio and FPR/IPC PR work split were utilized to maintain the optimal cycle efficiency. The ratio of top of climb to take-off power on-take was the same as proposed by Lents et al [18].

Sielemann [19] combined the two methods and produced a multi-point cycle design method. Even in [19], the mass flows are not conserved at top of climb. It can certainly be argued that a hybrid electric engine may perform better with a lower specific thrust cycle than a corresponding non-hybrid engine for the same thrust levels. But a comparison should be made also at the same specific thrust or fan diameter to isolate and benchmark the improvement in engine cycle efficiency without the nacelle skin friction drag penalty. Integration of power management strategies and engine cycle design for parallel hybrid engines has been presented in [16] and [23], but the individual benefits coming from these two are not quantified and no trade-offs are identified. Various aspects of engine cycle design, mission performance, and power management strategies have been discussed in the open literature

as summarized above, but still, some research questions have been left unanswered. They can be summarized as follows:

- What is the maximum benefit that can be obtained by redesigning the engine cycle with hybridization as compared to simply retrofitting the gas turbine with electrical power?
- What are the optimal motor power and battery sizes for a given mission range for minimization in fuel burn and energy consumption?
- Do the potential benefits from hybridization increase or decrease with improvement in gas turbine technology?

A novel integrated engine cycle design and power management strategy optimization methodology is developed and utilized to help answer the above-mentioned research questions for parallel hybrid electric architectures. It is important to address these research questions to provide a perspective of the maximum potential fuel burn benefit that can be expected from parallel HEPS architectures and the associated battery sizes and power management strategies. The impact of engine cycle design on the HEPS design space has not been explored thoroughly in the literature and as will be shown in this paper, it is an important factor in enabling electrification. The aircraft case study considered is a 110-seater single-aisle, regional aircraft, resembling the Fokker 100 [24] which is powered by two 2-spool fuselage-mounted turbofan engines Rolls Royce TAY 651 [25]. It is understood that the maximum benefits obtained from hybridization in terms of fuel burn are when the electrical motor is boosting the LP shaft of the gas turbine. The results indicate that retrofitting the gas turbine engine with hybridization (without modifying the engine) has turbine life benefits and marginal fuel burn benefits at lower ranges. Redesigning the gas turbine with hybridization has higher fuel burn benefits than the retrofit hybrid gas turbine case but no turbine life benefit relative to the baseline.

2. METHODOLOGY

An integrated aircraft-engine model has been developed to assess parallel hybrid electric aircraft performance. Cranfield University in-house aircraft performance code, ORION ([26], [27]) is used for the baseline aircraft weight, drag, and performance estimation and was extended to utilize different energy sources and to account for electrical powertrain weight and efficiency variation. Cranfield University in-house engine performance code, TURBOMATCH [31] and ATLAS [32] are used for baseline gas turbine cycle modeling and sizing respectively. ORION has been integrated with a solving scheme performing 3-point engine cycle design and optimization. It is also integrated with electric power management and aircraft mission optimization codes. Each of the individual elements of this methodology is described in this section. The parallel hybrid configuration examined in this study is presented in Figure 1.

2.1 ORION HEPS Workflow

ORION is similar in structure to NASA FLOPS [28]. The drag polar is based on empirical correlations from Raymer [29]. ORION employs the secant method to update the iteration variable in each internal mission loop and runs the loops till the error between two consecutive iteration variables is within convergence. These variables can either be fuel burn or range depending on the mission mode selected by the user. To avoid another internal iterative loop for battery and motor sizing, the battery and motors are sized externally. Once the battery weight and motor powers are defined throughout

the flight envelope, an internal state of charge calculator is embedded to discharge the battery only to 20% state of charge. A 4-D engine deck approach is developed to perform this task, where the specific fuel consumption, thrust, and fuel flow for each point are estimated as a function of thrust rating, motor power on-take, altitude, and Mach.

$$(tsfc, thrust, m_f) = f(alt, mach, ontake, \%thrust) \quad (1)$$

Genetic optimizer is employed to generate optimal power distribution for the electrical powertrain across the mission segments and is linked to the global aircraft performance loop in ORION. The variables, objective function, and constraints are given below in Table 1. The variables are the electrical power on-takes provided to the LP shaft for three flight mission segments - take-off, climb, and cruise. The variables can also be defined as a ratio of the electrical power on-take to the LP shaft power. All the flight mission phases (take-off, climb and cruise) are divided into many segments, and the battery state of charge is calculated at each segment. The motor power on-take is made zero if the battery state of charge falls below 20% during any segment. All the simulations were performed for a sweep of battery sizes and motor powers and within each simulation, a loop of GA optimizer was run to optimize the electrical power distribution across the flight mission. The battery stack sizing module was based on the SUGAR VOLT study [8] while the AC motor and inverter efficiency maps were developed from the method provided by Vratny et al [33]. The selection of the line voltage was kept at 1800 VDC based on the inputs from Vratny et al [33]. The cell characteristics are based on the Panasonic 20700A lithium-ion battery cell [36], and the battery parameters are reported in Table 2.

2.2 3-point engine cycle design approach

The approach developed for the hybrid cycle design is based on the baseline non-hybrid 3-point cycle design method from Guha [30] and Kyprianidis [38]. For a typical turbofan engine cycle, the top of climb mass flow sizes the fan diameter and take-off requirements and constraints size the core and bypass ratio. The cruise is kept as the design point and an SFC optimum cold stream to hot stream jet velocity ratio is targeted. Table 3 summarizes the approach utilized for the 3-point hybrid engine cycle design and the process is represented in Figure 2. As compared to a typical cycle design process, an extra variable of top of climb on-take is introduced as a parameter for hybridization. For all the cases, take-off power on-take is the maximum motor power available (coming from the degree of hybridization by power). No on-takes are provided for the design point (cruise).

For both the baseline and redesigned hybrid cases, the HPT blade metal temperatures are kept the same at take-off and top of climb. The main aim of redesigning the engine cycle is to exploit the flexibility provided by electrification by bringing the cruise operating point close to the thermal efficiency at take-off. Hence, no cruise on-take is applied while top of climb on-take is varied to exactly meet the HPT NGV and rotor blade metal temperatures during climb as the baseline. In such a way, the engine cycle is just about correctly sized to meet the temperature constraints. As discussed by Trawick [17], high continuous motor power is never recommended to avoid high discharge rates for the battery. Hence a continuous high motor rating is not used for all the flight segments and a variable power rating is used as required to meet the cycle requirements and constraints. The rest of the cycle design method is like the engine cycle design method described in [38]. The hybrid cycle design method consists of matching 10 design variables to corresponding parameters until convergence.

Secant method is employed to match the variables to the corresponding cycle parameters. The BPR is varied to meet the optimum jet velocity ratio, the OPR is varied to meet the T/O T30 constraint while maintaining the LPC/HPC work ratio at cruise and FPR is varied to meet the top of climb mass flows. The LPT spool speed is varied to meet the thrust at top of climb and take-off as depicted in Figure 2. The HPT NGV and rotor blade metal temperature constraints at take-off are met by varying the cooling flow fractions calculated according to Horlock [31]. Finally, the climb HPT NGV and rotor temperature of the hybrid engine is kept the same as the baseline by varying the climb motor power on-take.

2.3 Integrated hybrid aircraft-engine model

The developed methodology contains ORION aircraft performance model coupled with 3-point cycle design methodology, weight estimation, and electric powertrain performance. The models are integrated with a global optimizer. For weight estimation of the gas turbine, Cranfield University in-house code, ATLAS [32] is used. Physics-based motor and inverter efficiency models are employed, based on [33].

Figure 3 shows the top-level flow diagram for the optimal PMS and retrofit case. For the redesigned case study, the minimum value of top of climb and take-off power on-take is constrained by the blade metal temperature limits. It should be noted that the full flow diagram is only utilized when assessing the redesigned gas turbine case study integrated with optimal power management strategy. For the retrofit and optimal power management strategy cases, as no changes are made to the baseline engine, the 3-point engine cycle design code is not utilized.

3. RESULTS AND DISCUSSION

This section is divided into five segments: Baseline aircraft and engine, HEPS engine cycle design, HEPS aircraft mission assessment, HEPS EIS 2035 engine cycle design and HEPS aircraft mission assessment (EIS 2035). Section 3.1 provides information on the baseline aircraft and engine and validation data for the models developed. Section 3.2 describes the impact of electrification on the engine cycle design and summarizes the cycle data for baseline, retrofit, and redesigned cycles. Section 3.3 consists of the mission assessment results for all the hybrid cases utilizing the cycle design and power management optimization method. Section 3.4 provides engine cycle data for baseline, retrofit, and redesigned cases for EIS 2035 cycle constraints. Section 3.5 compares the impact of electrification across the full design space for the two engine technologies.

3.1 Baseline aircraft and engine

The aircraft model was developed in ORION using data from [34] while the engine model (inspired by TAY 651) was developed in TURBOMATCH and validated with [25]. The aircraft and engine model performance data can be summarized in Table 4. The payload-range capability was matched to public domain information [24] as depicted in Figure 4, indicating that the aircraft mission performance is predicted with good accuracy (<3%). The baseline engine data are provided in Table 5.

3.2 HEPS Engine Cycle Design

3.2.1 Retrofit engine cycle

The impact of electrification on the baseline engine is described in this sub-section. The retrofit engine simply means there is no change to the baseline engine and the engine is de-rated for the phases of flight where the motors provide power to the LP shaft. The retrofit hybrid engine will have potentially a turbine life benefit and NO_x reduction compared to the baseline due to the lower turbine work requirement and hence lower turbine entry temperatures. Figure 5 and Figure 6 show the drop in T40 and T30 on the same thrust level at take-off conditions with varying degrees of hybridization. Every 1 MW on-take leads to a drop in T40 by 41 K and a drop in T30 by 5 K. The retrofit engine data are provided in Table 5. This reduction in T40 and T30 gives some margin to redesign the cycle to smaller core sizes and higher OPRs at cruise. This will potentially lead to improvement in core efficiency and lower specific fuel consumption. Simultaneously, it will lead to higher core temperatures compared to the retrofit case, partly negating turbine life and NO_x benefit. An engine cycle redesigned to take advantage of this flexibility is presented in the next sub-section.

3.2.2 Redesigned engine cycle

In this subsection, the engine cycle that was redesigned with electrification is described. The method for engine cycle design described in section 2.2 is utilized to develop an engine cycle redesigned according to electrification. The comparison of the three engine cycles – baseline, retrofit, and redesigned hybrid is presented in Table 5. For the redesigned cycle, the power on-take is found to be 400 kW at top of climb to have the same blade temperatures as the baseline. All three cycles are compared at the same thrust levels as the maximum take-off weight constraint is maintained. For the redesigned hybrid case, the increase in design point BPR and OPR increases the thermal efficiency at cruise. Thereby reducing cruise specific fuel consumption by 0.7% relative to the baseline engine. The top of climb and cruise thrusts will be slightly different for the hybrid cycle depending on the power management strategies, but the differences are too small to be considered. The redesigned engine is also 7% lighter than the baseline engine due to the reduced core size. Though the ratio of top of climb to take-off on-take of 0.4 obtained from Figure 7 is not too different from Lents [18] (0.35), it heavily depends on gas turbine technology level and thrust ratios.

3.2.3 Gas turbine operability

In this subsection, the impact of electrification on gas turbine operability is described. In the last subsections, it was discussed that as the motor shaft power increases, there is a linear decrease in T40 and T30, which means a linear improvement in the cruise specific fuel consumption for the redesigned engine cycles with an increasing degree of hybridization. The maximum power provided at take-off, climb and cruise though will ultimately be limited by the impact on the operability of the gas turbine components. The LPC moves towards surge on application of on-take for any phase of flight. This is

particularly more prominent if higher motor power is provided to the LP shaft as seen in Figure 8. The HPC operating point change with power on-take is shown in Figure 9. If the HP shaft was powered instead of the LP shaft, the trend is reversed and shown in [11]. Operating characteristics will remain the same for redesigned engine cycle as the retrofit as the cruise design point surge margin is kept the same and no electrification is provided at that point. The gas turbine can certainly be redesigned keeping the surge margin of the compressors in mind with electrification but that would also reduce the specific fuel consumption benefit. Hence, the cruise surge margin is kept the same.

The ratio of top of climb to take-off power of 0.40 is ideal from an engine cycle design and operability point of view but is not ideal from a power management strategy point of view. The power distribution for the retrofit hybrid would depend on three factors: variation of aircraft weight due to change in on-takes, battery discharge rates, and motor-inverter efficiency. From the battery stack model described in Section 2.1, higher discharge rates/ currents will reduce the efficiency of the battery, keeping the discharge rate low is a critical factor for both performance and life. The variation in motor-inverter efficiency with power is typically low, from models described in section 2.1. It can be concluded that the battery discharge rates, and aircraft weight variation are driving factors in the selection of a power management strategy. Hence, the ideal power management strategy would be to utilize a fraction of the maximum available power throughout the flight, powering mostly cruise, to have lower battery discharge rates and get lighter earlier in the mission. However, such a distribution will have operability issues at cruise and would give limited scope for engine core reduction.

3.3 HEPS aircraft mission assessment

This section presents the mission performance results for HEPS engine cycles described in the earlier section. It is divided into two sub-sections: Fixed battery energy and Sweep of battery weights.

3.3.1 Fixed battery energy

In this sub-section, a comparison is made between redesigned and retrofit hybrid cycles for a set of off-design mission ranges in terms of fuel burn and energy consumption using the cycle data summarized in Table 5. These are performed with current assumptions on the electrical powertrain and a sweep of battery energy densities with fixed battery energy, sized to provide 1 MW during take-off and climb. The complete powertrain efficiency (battery, motor, and inverter) considered for the design point is 0.86, with no superconducting technology considered for the electrical motors. The electrical powertrain and thermal management power densities are summarized in Table 6 for both state of the art and 2035 assumptions. The 2035 assumptions on the power densities are used to produce the results in section 3.3.2. In this study, the weights for the thermal management systems are considered. It can be seen from Figure 10, that payload needs to be reduced with an increase in mission range to meet the ramp weight constraint for mission ranges above 1000 nm and all energy densities considered. For battery energy density of 250 Wh/kg, there is a consistent penalty in the payload for all mission ranges considered except for missions shorter than 400 nm.

There is no penalty in payload till 1000 nm for 750 Wh/kg for both retrofit and redesigned case studies. It is observed that the redesigned hybrid case results in lower penalty in payload than the retrofit hybrid for all mission ranges. This is attributed to 7% lower engine weight and lower specific fuel

consumption. Two new parameters are defined to compare energy and fuel economy, accounting for the penalty in payload and range, named as Normalized delta energy and Normalized delta fuel.

$$\text{Normalized Energy} = \frac{\text{Energy consumption}}{(\text{Range} * \text{pax})} \quad (2)$$

$$\text{Normalized Fuel} = \frac{\text{Fuel consumption}}{(\text{Range} * \text{pax})} \quad (3)$$

In Figure 11 and Figure 12, to separate benefits arising from cycle design and power management strategy, a continuous 1 MW on-take till battery discharges, is provided for both retrofit and redesign. Figure 11 and Figure 12 show the percentage difference in Normalized Energy and Normalized Fuel respectively between HEPS architectures (retrofit and redesign) and baseline engine. It is seen that even with a 750 Wh/kg assumption on the battery energy density, there is no benefit in normalized fuel burn for retrofit hybrid design relative to the baseline non-hybrid for all mission ranges. The same trend is observed in normalized energy consumption relative to the baseline, with penalties ranging from 0.2% to 36%. The redesign brings a benefit of the order of 1-1.1% in block fuel burn relative to retrofit for all ranges with the maximum payload. On a mission range of 400 nm, the redesigned provides a 1.8% fuel burn benefit relative to the baseline. Since the Fokker 100 flies 50% of the flights below 400 nm, there is scope for fuel burn improvement with a properly designed engine cycle, optimally sized thermal management systems and optimally utilized electric powertrain. The comparison of the same redesigned cycle with these two different power distributions is described further in section 3.3.2.

3.3.2 Sweep of battery weights

The next set of simulations is performed to identify the appropriate battery size and motor power for this aircraft using battery energy density of 750 Wh/kg and 2035 estimates on the electric powertrain. As the battery size increases, the maximum payload range of the aircraft reduces due to added weight and the energy consumption penalty also increases. In all the flight mission results considered herein, the genetic algorithm optimizer is employed to optimize the electrical power distribution along the flight mission. This is integrated and utilized with the cycle design method for the redesigned case studies. The line 'Battery limited by power' in Figure 13 is the maximum range below which the battery is not fully discharged (SoC>20%) and is oversized. This is a key parameter that reflects the need for a higher motor power to discharge the battery for lower flight mission ranges. The line 'Battery limited by MTOW' highlights the maximum flight mission range for maximum payload for different battery weights. Figure 14 illustrates the potential benefit arising from simply utilizing the battery in a more favorable manner without any cycle redesign. The maximum fuel burn benefit from optimizing the power management strategy is approximately 0.2-0.3%, which is less than the benefit from cycle redesign. Optimal power management strategy suggests an almost continuous low power value of motor to get a balance between aircraft weight and battery resistance effect.

The final comparison is made between 0.5 and 1 MW motor power for the sweep of battery sizes in Figure 15 and Figure 16. It is seen that retrofit hybrid with 0.5 MW consumes less block energy and

fuel than 1 MW for the same battery size, but the trend is the opposite for redesigned hybrid. This shows that core size reduction has a more pronounced effect on fuel burn and energy consumption than electrical powertrain weight increment for the same battery size. A higher motor power on-take will improve the fuel burn benefit due to greater margin to redesign the engine cycle but will have operability issues and higher cruise turbine entry temperatures. The 1 MW redesigned hybrid has a roughly 45 K higher T40 than the baseline engine, while the 0.5 MW redesigned hybrid has roughly 22 K higher T40 than the baseline engine at cruise. This leads us to the conclusion that a higher power on-take would enable higher fuel burn benefits for redesigned cycles for the given case study. However, this power on-take may ultimately be limited by cruise turbine entry temperatures in cases where a higher margin for cycle redesign is available.

Finally, some light is shone on different power management strategies for the redesigned engine cycle. The difference between redesigned and retrofit delta energy is slightly higher for the results shown in Figure 11 than Figure 16 by 0.2% corresponding to a battery size of 1153 kg. This difference is due to the better power management strategy of 1 MW and 400 kW at take-off and top of climb instead of 1 MW throughout, till the battery discharges. The identification of optimal battery size is heavily dependent on the operation of the aircraft fleet. It is seen from Figure 17 and Figure 18 that a 2307 kg battery pack has greater fuel burn benefit than an 1153 kg battery pack for all ranges below 800 nm but has a reduced maximum payload range capability by almost 300 nm.

3.4 HEPS EIS 2035 engine cycle design

The TAY 651 hybrid results have been presented in the earlier sub-chapters. TAY 651 has been in service since 1990 [25] hence when hybridization will be applied, more efficient gas turbines will be available for the same thrust class. The next step would be to analyse the impact of hybridization for a modern UHBR geared turbofan engine with polytropic efficiency estimates for EIS 2035[35]. In this section, hybrid engine cycle design is performed and presented for an entry into service 2035 turbofan engine. The engine cycle design and aircraft mission assessment methods are the same as described in the previous chapters. The engine cycle parameters are summarized in the Table 7. For the same electrical input power of 1 MW, the redesign cruise specific fuel consumption benefit is 0.92% relative to the retrofit cycle. It should be noted that this is an optimum cycle without putting constraints on the blade height of last stage of the HPC, which may put the baseline cycle at a lower OPR and T40.

This is slightly higher than the specific fuel consumption benefit which was obtained for the TAY redesign relative to retrofit. This brings us to a more fundamental understanding of parallel hybrid turbofan systems. It is intuitive to think that as the thermal efficiency of the gas turbine increases, the delta fuel burn percentage benefit of parallel hybrid electric systems should reduce. But the reduction in specific thrust has a greater impact than the improvement in thermal efficiency. Hence, for the same electrical power, there is a greater contribution to thrust from the electrical powertrain as lower specific thrust dominates thermal efficiency. This is the reason why EIS 2035 engine shows greater reduction in specific fuel consumption as compared to TAY 651 on application of same electrical power on-take.

3.5 HEPS Aircraft mission assessment

The hypothesis proposed in the previous subsection is more easily understood from the mission-level assessment. To cover the full design space for parallel hybrids, two specific parameters are used. These are H_P and H_E , called degree of hybridization by power and degree of hybridization by energy.

$$H_P = \frac{P_{motor}}{P_{shaft}} \quad (4)$$

$$H_E = \frac{E_{bat}}{E_{mission}} \quad (5)$$

Figure 19 shows the percentage delta fuel burn between hybrid retrofit TAY (hTAY) and baseline TAY (cTAY) on 500 nm. For 5% H_P and 4% H_E , the fuel burn benefit is 1.91% with a total battery weight of 2167 kg. Figure 20 shows the percentage of delta fuel burn between hybrid retrofit EIS 2035 and conventional EIS 2035. For the same 5% H_P and 4% H_E , the percentage fuel burn benefit is 2.58% with a total battery pack weight of 1321 kg.

From these two contour plots, for the same H_P and H_E , hybrid EIS2035 has a greater fuel burn benefit than hybrid TAY relative to their respective basely baseline engines. This is reflected in the LP shaft power, as it reduces from 16 to 10 MW approximately from the TAY to EIS 2035. For the same H_P and H_E , hybrid EIS 2035 requires lighter battery and motor weights due to two reasons, lower shaft power requirement and higher shaft speed. The maximum LP shaft speed of the EIS 2035 is 11,200 RPM while TAY 651 is 8800 RPM [25]. The battery weights are only affected by the lower shaft power requirement and not the motor rotational speeds as line voltages are the same. The contribution of a higher motor power-to-weight ratio is much lower than the contribution of LP shaft power reduction to the fuel burn benefit for EIS 2035. The reduction in motor and inverter weights due to higher shaft speeds is only around 40 kg so it is safe to assume most of the fuel burn benefit for the hybrid EIS 2035 as compared to hybrid TAY 651 comes from the lower shaft power requirement. Reduction in weights mainly due to lower shaft power requirement means that less fuel burn penalty is paid to carry the dead weight in the case of EIS 2035, and this is reflected in delta mission fuel burn in Figure 20. The trend of the energy burn is similar in both cases and is shown below in Figure 21 and Figure 22. But it can be seen even in energy burn, hybrid EIS 2035 has a significantly lower energy penalty than hybrid TAY. Figure 17 showed that 2-5% fuel burn can be saved with a 2307 kg battery pack on a redesigned TAY. Since the benefit is 0.7-0.8% more on a hybrid redesigned EIS 2035 (difference between Figure 19 and Figure 20), the total benefit jumps to approximately 3-6%.

4. CONCLUSION

This work presented a comprehensive mission assessment and design methodology for parallel HEPS systems for single-aisle aircraft applications. The results were presented for retrofit, optimal PMS, and redesigned engine cycle case studies with varying motor powers and battery sizes across several mission ranges. It has been demonstrated the improvement in fuel burn benefit from hybridization increases with reduction in engine specific thrust. The major conclusions from this study can be summarized as follows:

- Low engine specific thrust and high battery energy density are driving factors for reduction in fuel burn for HEPS
- There is only a benefit of 1.8% fuel burn at 400 nm for Fokker 100 – hybrid TAY with a battery energy density of 750 Wh/kg, sized for T/O & Climb, current power density estimates on the motor, inverter, and thermal management system.
- Improvement in electrical powertrain density and implementing on a modern UHBR engine shows a much bigger fuel burn benefit ranging from 3-6% across full design space relative to the baseline engine.
- Low H_E and high H_P is the most suitable combination for fuel burn and energy consumption reduction.
- Power management strategies do not have a particularly big benefit at the aircraft level mission fuel burn but are critical from the point of view of the aircraft-engine operation and battery life.
- The cruise specific fuel consumption benefit obtained from redesigning the engine cycle with hybridization of 1 MW power on the TAY 651 engine is around 0.7% which translates into 1.1% fuel burn benefit taking the reduced engine weight into account.
- The maximum motor power into the shaft may ultimately be limited by the turbine entry temperature at cruise with the redesigned cycle.

This work provides a perspective, of the fuel burn benefit that can be expected from parallel HEPS architectures from different engine cycle design technology scenarios. It also provides a robust, integrated method to perform engine cycle design with power management strategy optimization and mission assessment of these architectures. The method is flexible and can be easily modified to assess other HEPS configurations on different aircraft classes.

ACKNOWLEDGEMENTS

The authors are grateful to Rolls Royce plc for the funding and technical support on this research and granting permission to publish this paper.

REFERENCES

- [1] M. Darecki and C. Edelstenne, "Flightpath 2050 Europe's vision for aviation: Report of the high level group on aviation research," Isbn 978-92-79-19724-6, p. 28, 2011, doi: 10.2777/50266.
- [2] J. Whurr and J. Hart, "A Rolls-Royce Perspective on Concepts and Technologies for Future Green Propulsion Systems," *Encycl. Aerosp. Eng.*, pp. 1–9, 2015, doi: 10.1002/9780470686652.eae1020.
- [3] E. Partnership, "Strategic Research and Innovation Agenda," p. 154, December 2021.
- [4] NASA, "Hybrid Thermally efficient Core (HyTEC)." <https://www1.grc.nasa.gov/aeronautics/hytec/> (updated Dec. 22, 2020).
- [5] C. Goldberg, "Techno-economic, Environment and Risk Analysis of an Aircraft Concept with Turbo-electric Distributed Propulsion", PhD Thesis, Dec 2017, Cranfield University.
- [6] J. L. Felder, H. D. Kim, and G. V. Brown, "Turboelectric distributed propulsion engine cycle analysis for hybrid-wing-body aircraft," 47th AIAA Aerosp. Sci. Meet. Incl. New Horizons Forum Aerosp. Expo., pp. 1–25, 2009, doi: 10.2514/6.2009-1132.
- [7] K. P. Duffy, "Turboelectric and Hybrid Electric Aircraft Drive Key Performance Parameters AIAA Electric Aircraft Technologies Symposium," *AIAA Electr. Aircr. Technol. Symp.*, pp. 1–23, 2018, [Online]. Available: <https://ntrs.nasa.gov/search.jsp?R=20180007414>.
- [8] M. K. Bradley, T. J. Allen, and C. K. Droney, "Subsonic Ultra Green Aircraft Research: Phase II – Volume II – Hybrid Electric Design Exploration," *NASA Tech. Rep.*, vol. CR–2015-21, no. April, p. 76, 2015.
- [9] C. E. Lents, "Impact of Weight, Drag and Power Demand on Aircraft Energy Consumption," *AIAA Propulsion and Energy Forum.*, pp. 1–6, 2021, doi: 10.2514/6.2021-3322.
- [10] C. A. Saias, I. Goulos, I. Roumeliotis, V. Pachidis, and M. Bacic, "Preliminary Design of Hybrid-Electric Propulsion Systems for Emerging Urban Air Mobility Rotorcraft Architectures," *J. Eng. Gas Turbines Power*, vol. 143, no. 11, 2021, doi: 10.1115/1.4052057.
- [11] K. R. Antcliff, "Mission Analysis of Hybrid Electric Regional Aircraft," *AIAA SciTech Forum*, no. January, pp. 1–18, 2016.
- [12] G. Cinar, "A Methodology for Dynamic Sizing of Electric Power," PhD Thesis, Georgia Institute of Technology, no. December, pp. 1–366, 2018.
- [13] J. Thauvin, G. Barraud, M. Budinger, D. Leray, X. Roboam, and B. Sareni, "Hybrid regional aircraft: A comparative review of new potentials enabled by electric power," 52nd AIAA/SAE/ASEE Jt. Propuls. Conf. 2016, 2016, doi: 10.2514/6.2016-4612.
- [14] D. F. Finger, C. Braun, and C. Bil, "Comparative assessment of parallel-hybrid-electric propulsion systems for four different aircraft," *AIAA Scitech 2020 Forum*, vol. 1 PartF, no. January, 2020, doi: 10.2514/6.2020-1502.
- [15] C. Pornet, "Conceptual Design Methods for Sizing and Performance of Hybrid-Electric Transport Aircraft," p. 144, 2018.

- [16] C. Perullo, D. Trawick, M. Armstrong, J. C. M. Tai, and D. N. Mavris, "Cycle selection and sizing of a single-aisle transport with the Electrically Variable Engine (EVE) for fleet level fuel optimization," AIAA SciTech Forum - 55th AIAA Aerosp. Sci. Meet., no. January, pp. 1–17, 2017, doi: 10.2514/6.2017-1923.
- [17] D. R. Trawick, "A Methodology for the Determination of Optimal Operational Schedules of Hybrid Electric Architectures," no. May, pp. 1–228, 2018.
- [18] C. Lents, L. Hardin, J. Rheume, and L. Kohlman, "Parallel hybrid gas-electric geared turbofan engine conceptual design and benefits analysis," 52nd AIAA/SAE/ASEE Jt. Propuls. Conf. 2016, pp. 1–12, 2016, doi: 10.2514/6.2016-4610.
- [19] S. Sahoo, K. Kyprianidis, and X. Zaho, "Performance assessment of an integrated parallel hybrid-electric propulsion system aircraft," in ASME Turbo Expo 2019, 2019, pp. 8–12.
- [20] M. Sielemann, C. Coïc, X. Zhao, D. E. Diamantidou, and K. Kyprianidis, "Multi-point design of parallel hybrid aero engines," AIAA Propuls. Energy 2020 Forum, pp. 1–18, 2020, doi: 10.2514/6.2020-3556.
- [21] Kang S, Roumeliotis I, Zhang J, Broca O & Pachidis V (2022) Assessment of engine operability and overall performance for parallel hybrid electric propulsion systems for a single-aisle aircraft, Journal of Engineering for Gas Turbines and Power, Volume 144, Issue 4, Article number 041002.
- [22] R. de Vries, M. T. Brown, and R. Vos, "A preliminary sizing method for hybrid-electric aircraft including aero-propulsive interaction effects," 2018 Aviat. Technol. Integr. Oper. Conf., 2018, doi: 10.2514/6.2018-4228.
- [23] A. Seitz, M. Nickl, A. Stroh, and P. C. Vratny, "Conceptual study of a mechanically integrated parallel hybrid electric turbofan," Proc. Inst. Mech. Eng. Part G J. Aerosp. Eng., vol. 232, no. 14, pp. 2688–2712, 2018, doi: 10.1177/0954410018790141.
- [24] D. Posted et al., "Aircraft - Fixed-Wing - Civil - Fokker 100," 2019.
- [25] Jane's, "Jane's Aero Engines," 2018.
- [26] P. Rompokos, S. Kisson, I. Roumeliotis, D. Nalianda, T. Nikolaidis, and A. Rolt, "Liquefied natural gas for civil aviation," Energies, vol. 13, no. 22, 2020, doi: 10.3390/en13225925.
- [27] S. Kisson, F. S. Mastropierro, D. K. Nalianda, A. Rolt, and B. Sethi, "Assessment of the BWB aircraft for military transport," Aircr. Eng. Aerosp. Technol., vol. 92, no. 5, pp. 769–776, 2020, doi: 10.1108/AEAT-09-2019-0188.
- [28] T. M. Lavelle and B. P. Curlett, "Aircraft Performance and Sizing Code," no. October, 1994.
- [29] D. Raymer, Aircraft Design: A Conceptual Approach, Sixth Edition. 2018.
- [30] A. Guha, D. Boylan, and P. Gallagher, "Determination of optimum specific thrust for civil aero gas turbine engines: A multidisciplinary design synthesis and optimisation," Proc. Inst. Mech. Eng. Part G J. Aerosp. Eng., vol. 227, no. 3, pp. 502–527, 2013, doi: 10.1177/0954410011435623.
- [31] J. H. Horlock and W. W. Bathie, Advanced Gas Turbine Cycles, vol. 126, no. 4. 2004.
- [32] P. Lolis, "Development of a Preliminary Weight Estimation Method for Advanced Turbofan Engines," Cranf. Univ. PhD Thesis, no. July, p. 214, 2014,

<https://core.ac.uk/download/pdf/29409793.pdf><https://dspace.lib.cranfield.ac.uk/handle/1826/9244>.

- [33] P. C. Vratny, C. Gologan, C. Pernet, A. T. Isikveren, and M. Hornung, "Battery Pack Modeling Methods for Universally-Electric Aircraft," *Ceas* 2013, pp. 525–535, 2013.
- [34] Jane's, "Jane's all the world's aircrafts," 2018.
- [35] K. G., "Future Aero Engine Designs: An Evolving Vision," *Adv. Gas Turbine Technol.*, no. June, 2011, doi: 10.5772/19689.
- [36] Panasonic, "NCR20700A data sheet," 2020.
- [37] C. A. Saias, I. Roumeliotis, I. Goulos, V. Pachidis, and M. Bacic, "Design Exploration and Performance Assessment of Advanced Recuperated Hybrid-Electric Urban Air Mobility Rotorcraft," *J. Eng. Gas Turbines Power*, vol. 144, no. 3, pp. 1–11, 2022, doi: 10.1115/1.4052955.
- [38] K. Kyprianidis, "Multi-disciplinary conceptual design of future jet engine systems", PhD Thesis, April 2010, Cranfield University.

Accepted Manuscript Not Certified

TABLES

Table 1 - Genetic Optimizer

Objective Function	Min fuel burn
Variables	<ul style="list-style-type: none"> • Take-off on-take • Climb on-take • Cruise on-take
Constraints	<ul style="list-style-type: none"> • Aircraft TOW • Battery SoC > 20%

Table 2 - Battery characteristics

Nominal Cell Voltage (V)	3.6
SoC (%)	20
Specific Energy Density (Wh/kg)	250
Specific Power (kW/kg)	1.2
Capacity (Ah)	3.3

Table 3 – 3-point cycle design parameters and variables

Objective function	Min tsfc
Design parameters	<ul style="list-style-type: none"> • Cruise thrust • Top of climb thrust • Take-off thrust • T/O T30 • T/O T40 • Top of climb Tblade • Top of climb mass flow • Cruise jet velocity ratio • Cruise IPC/HPC work split • End of runway Tblade
Variables	<ul style="list-style-type: none"> • Cruise FPR • Cruise BPR • Cruise T40 • Cruise LPC PR • Cruise HPC PR • Cruise mass flow • Top of climb power on-take • Top of climb LPT spool speed • Take-off LPT spool speed • Cooling fractions

Table 4 - Fokker 100 aircraft & engine data

Max Ramp Weight (kg)	45909
Max Payload Range (nm)	1425
Max Payload (kg)	10750
Cruise tsfc (g/kN.s) (TAY 651)	19.47
Cruise BPR (-)	3.06
SLS Thrust (kN)	68.5
T/O T40 (K)	1411

Table 5 - Comparison of baseline, retrofit hybrid and redesigned hybrid engine cycles

Parameter	Baseline	Retrofit, delta		Redesigned, delta	
Cruise BPR (-)	3.06	3.06	0	3.329	8.8%
Cruise tsfc (g/kN.s)	19.475	19.475	0	19.34	-0.7%
Cruise OPR (-)	16.6	16.6	0	17.01	2.5%
Cruise T40 (K)	1160	1160	0	1198	38
T/O T40 (K)	1411	1369	-42	1411	0
T/O T30 (K)	728	723	-5	728	0
Top of climb mass flow (kg/s)	80.26	80.85	0.7%	80.26	0
Cruise on-take (kW)	0	0	0	0	0
Top of climb on-take (kW)	0	400	400	400	400
T/O on-take (kW)	0	1000	1000	1000	1000

Table 6 - Electrical powertrain assumptions

Parameter	Current	2035
Motor Power density (kW/kg)	7	13
Inverter Power density (kW/kg)	11	19
Thermal Management Power density (kW/kg)	0.7	1.2
Battery Power Density (kW/kg)	1.2	2

Table 7 - EIS 2035 Engine cycle parameters

Parameter	Baseline	Retrofit, delta		Redesigned, delta	
Cruise BPR (-)	17.5	17.5	0	18.6	6.2%
Cruise tsfc (g/kN.s)	12.95	12.95	0	12.83	-0.9%
Cruise OPR (-)	52.44	52.44	0	54.79	4.5%
Cruise T40 (K)	1630	1630	0	1677	47
T/O T40 (K)	1880	1824	-56	1880	0
T/O T30 (K)	946	934	-12	946	0

Top of climb mass flow (kg/s)	165.09	165.43	0.2%	165.09	0
Cruise on-take (kW)	0	0	0	0	0
Top of climb on-take (kW)	0	400	400	400	400
T/O on-take (kW)	0	1000	1000	1000	1000

FIGURES

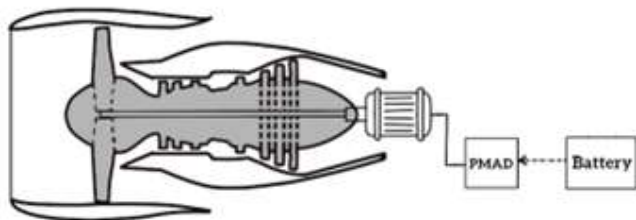


Figure 1 - Parallel HEPS Schematic

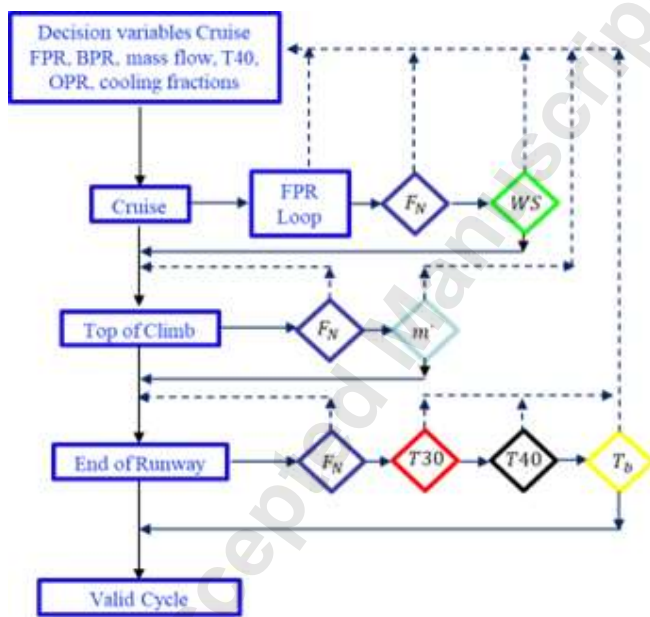


Figure 2 - 3-point cycle design flowchart

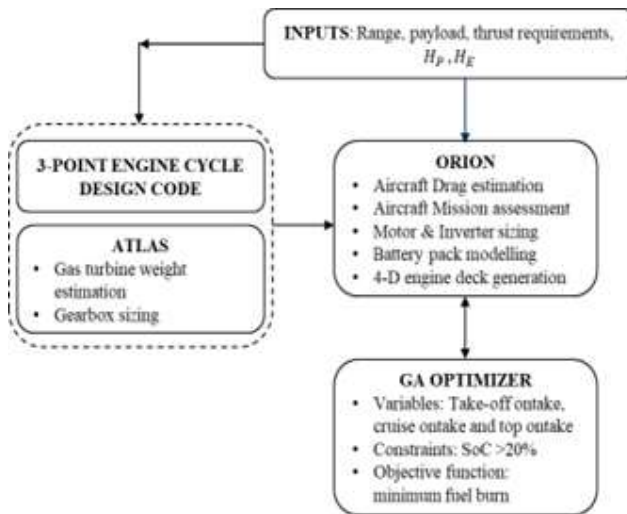


Figure 3 - Top-level flow diagram

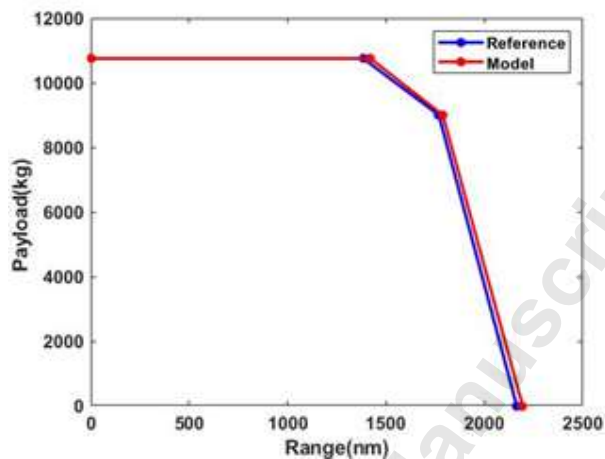


Figure 4 - Payload range diagram validation with [24]

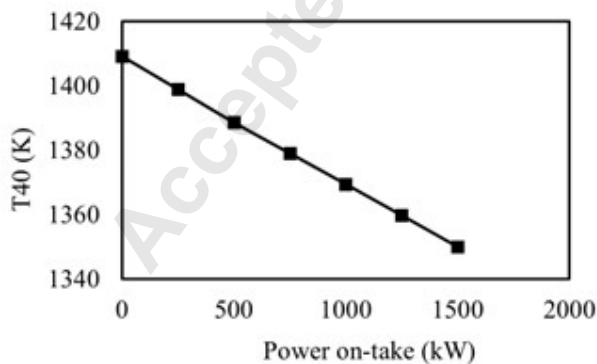


Figure 5 - Variation in T40 with power on-take at EOR on same thrust level

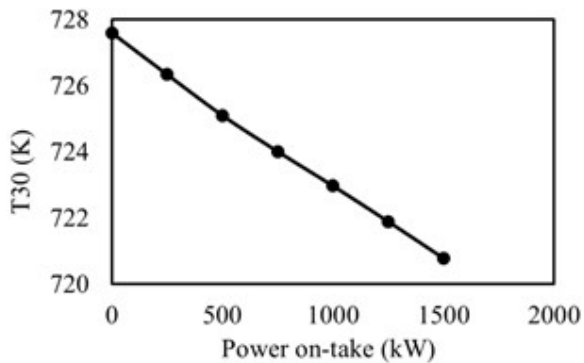


Figure 6 - Variation in T30 with power on-take at EOR on same thrust level

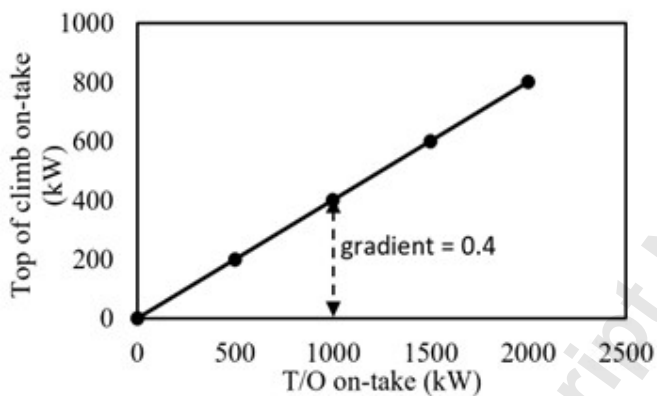


Figure 7 - Power on-takes for T/O and top of climb

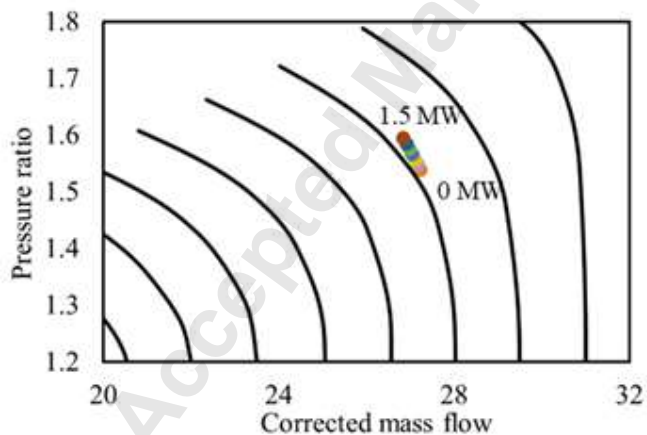


Figure 8 - LPC operability vs on-take at EOR

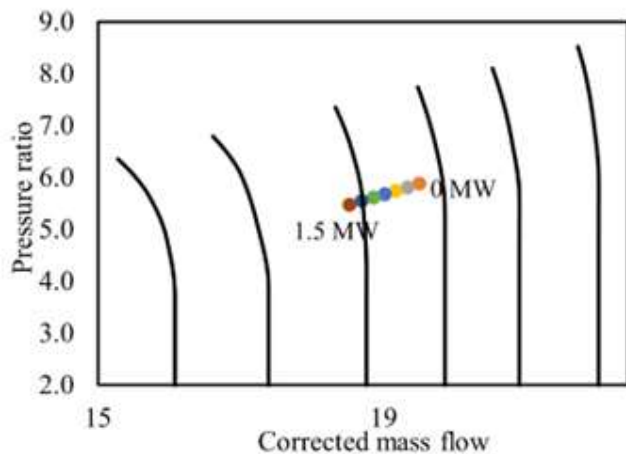


Figure 9 - HPC operability vs on-take at EOR

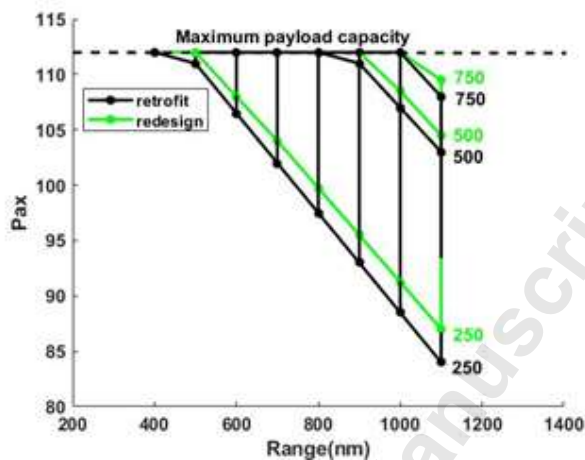


Figure 10 - Payload vs battery energy densities for range of ranges

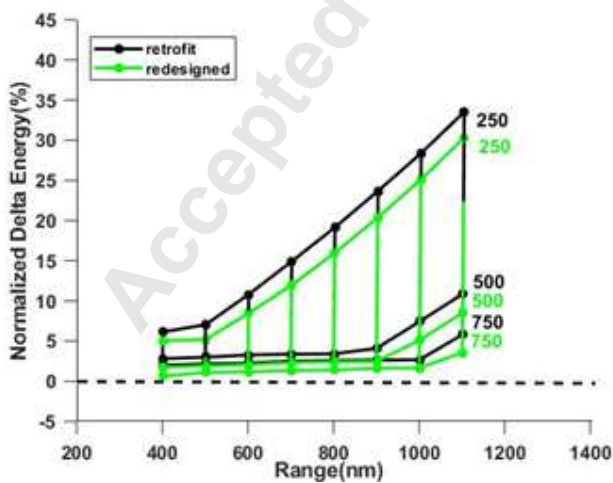


Figure 11 - Normalized delta energy (%)

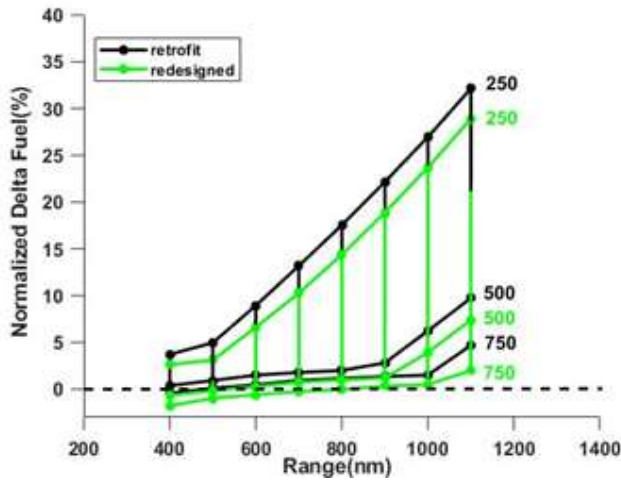


Figure 12 - Normalized delta fuel (%)

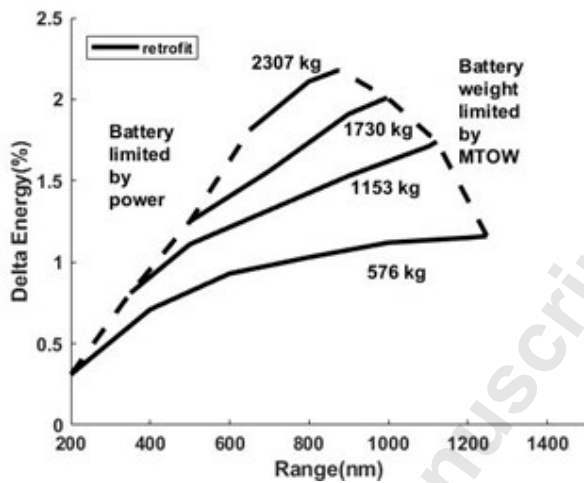


Figure 13 - Battery weights vs range of ranges sweep for 0.5 MW retrofit

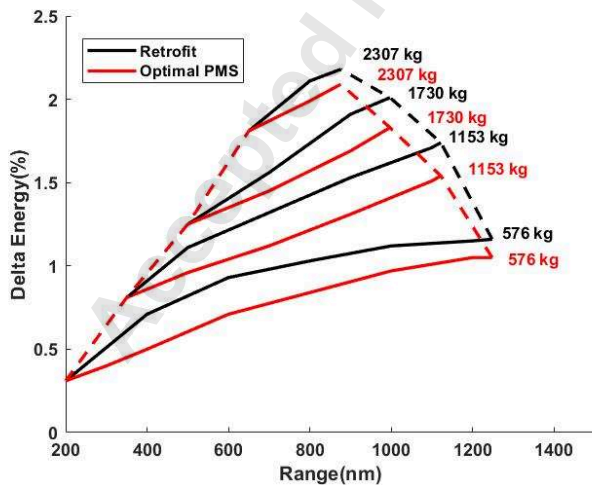


Figure 14 - Retrofit vs Optimal PMS

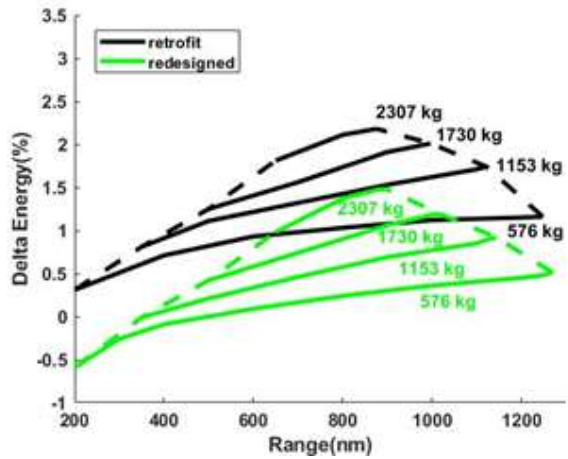


Figure 15 - Delta energy % for 0.5 MW

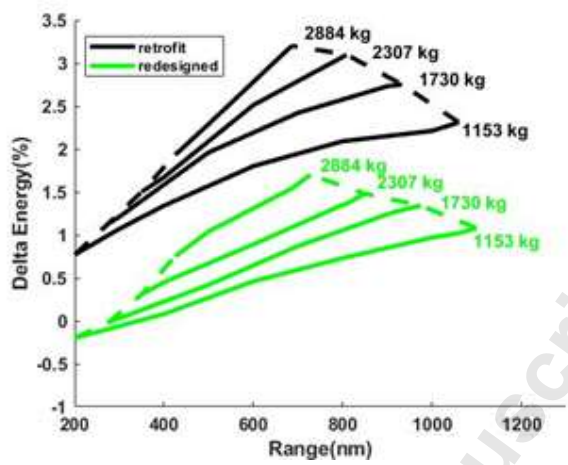


Figure 16 - Delta energy % for 1 MW

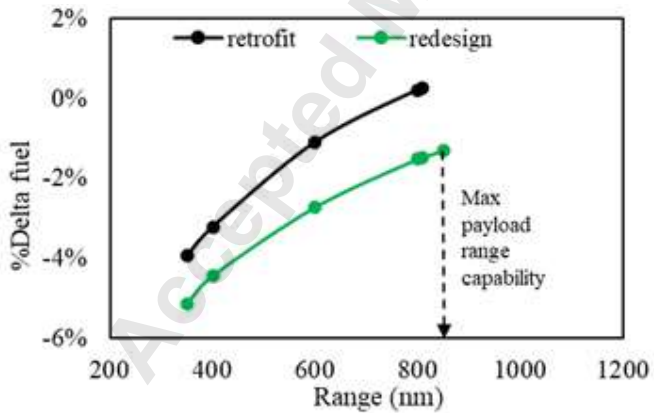


Figure 17 - % Delta fuel for 2307 kg battery pack

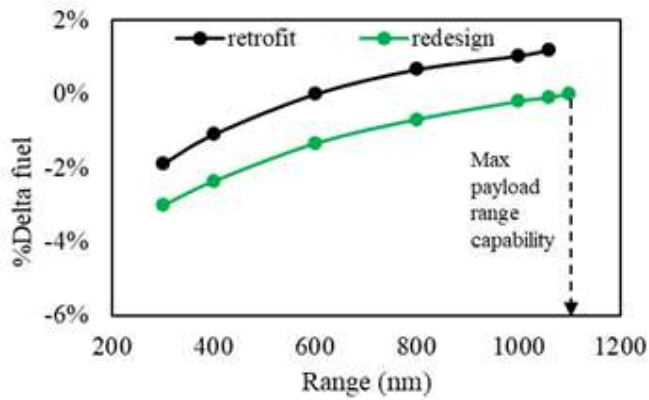


Figure 18 - % Delta fuel burn for 1153 kg battery pack

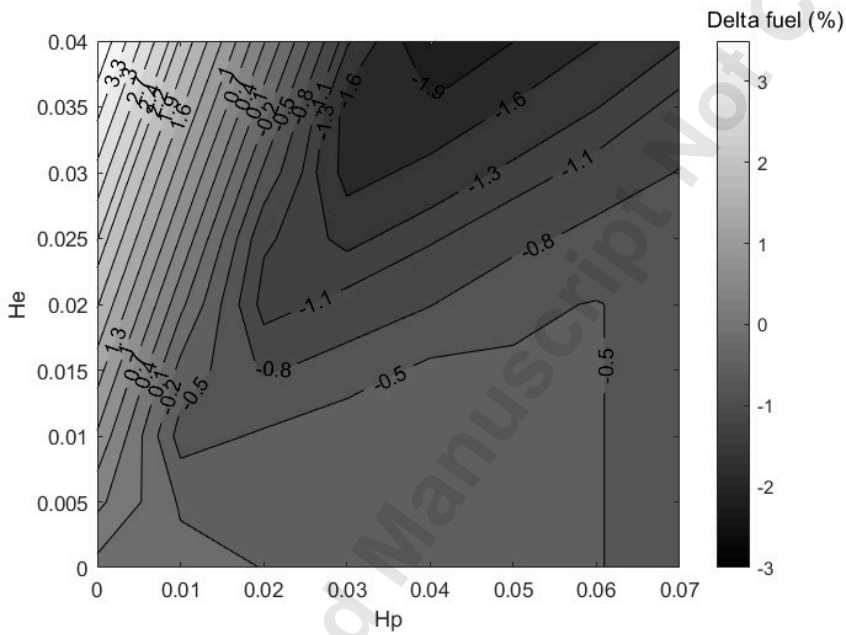


Figure 19 - % Delta fuel burn hTAY vs cTAY

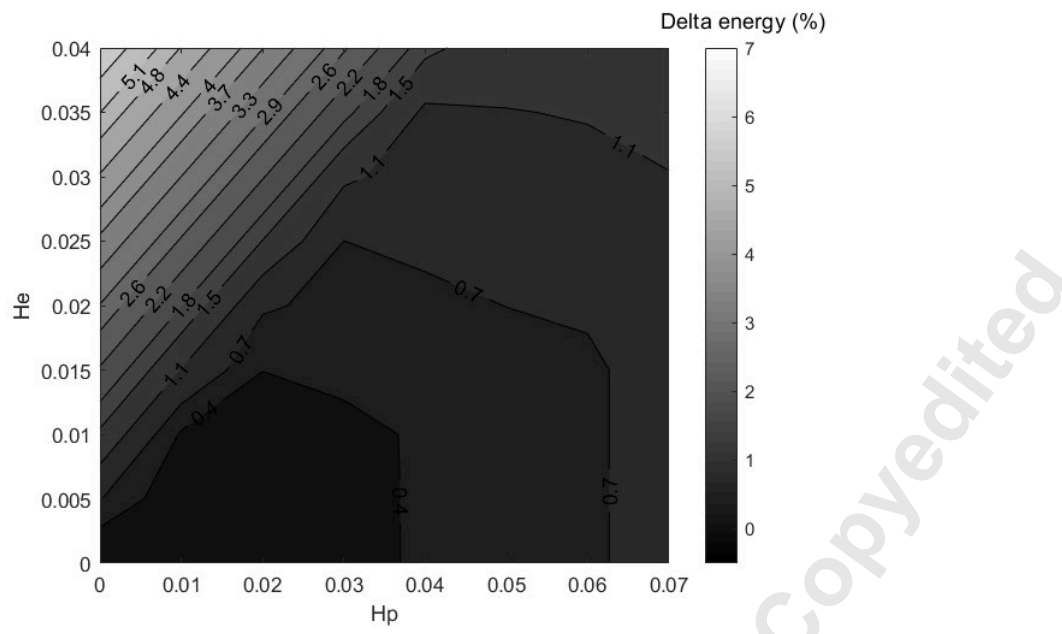


Figure 22 - Delta energy burn (%), hybrid EIS2035 vs conventional EIS2035

Accepted Manuscript Not Copyedited